

THE X-RAY FACILITY OF THE PHYSICS DEPARTMENT OF THE FERRARA UNIVERSITY

G. LOFFREDO^{1,*}, F. FRONTERA^{1,3}, D. PELLICCIOTTA¹, A. PISA¹, V. CARASSITI²,
S. CHIOZZI², F. EVANGELISTI², L. LANDI², M. MELCHIORRI²
and S. SQUERZANTI²

¹Physics Department, University of Ferrara, via Saragat 1, I-44100, Ferrara, Italy; ²Istituto Nazionale di Fisica Nucleare, Sezione di Ferrara, Ferrara, Italy; ³IASF, CNR, Via Gobetti 101, Bologna, Italy

(*author for correspondence, e-mail: loffredo@fe.infn.it)

(Received 17 February 2005; accepted 9 June 2005)

Abstract. We will report on the equipment and performance of the X-ray facility of the University of Ferrara. Initially developed to test the PDS (Phoswich Detection System) instrument aboard the BeppoSAX satellite and to perform reflectivity measurements of mosaic crystal samples of HOPG (Highly Oriented Pyrolytic Graphite), with time the facility has been improved and its applications extended. Now these applications include test and calibration of hard X-ray (>10 keV) detectors, reflectivity measurements of hard X-ray mirrors, reflectivity tests of crystals and X-ray transparency measurements. The facility is being further improved in order to determine the optical axis mosaic crystals in Laue configuration within a project devoted to develop a hard X-ray (>60 keV) focusing optics (Pisa, A. et al.: in press, Feasibility study of a Laue lens for hard X-rays for space astronomy, *SPIE Proc.*, 5536).

Keywords: astronomy, diffractometer, instrumentation, X-ray

1. Introduction

Many astrophysical phenomena are accessible only observing the celestial sources in hard X-rays (>10 keV), as shown by several X-ray satellite missions, like BeppoSAX, Rossi XTE, INTEGRAL, and the just launched SWIFT mission devoted to Gamma Ray Bursts. Also the next missions, like ASTRO-E2 will include hard X-ray detector. Thus far these telescopes are based on hard X-ray detectors, that view the sky, through or not, coded masks.

However there is a general consensus that the next generation of hard X-ray (>10 keV) telescopes will include focusing optics. Only with these optics it is possible to improve, by orders of magnitude, the sensitivity of the direct-viewing instruments. The focusing techniques, with multilayers ($E < 70$ keV) or with mosaic crystals ($E > 70$ keV), are in an advanced stage of development, specially in the case of multilayer mirrors. Indeed missions based on multilayers have already been proposed (e.g., NeXT, Takahashi et al., in press; HEXIT-SAT, Fiore et al., in press). Even hard X-ray missions based on the traditional external

reflection from high Z materials but with very long focal length (>30 m) have been proposed (SIMBOL-X).

Accurate test and calibration of these focusing telescopes are crucial in order to correctly derive their response function and thus to avoid systematic errors in the determination of spectral, temporal and energetic properties of the X-ray celestial sources. In order to perform these calibrations, monochromatic and parallel X-ray beams are desired. The beam energies have to cover the energy passband of these new telescopes (up to several hundreds of kilo electronvolts).

To this end, either for testing or for calibrating the hard X-/gamma-ray mirrors under development, suitable hard X-ray facilities are needed. The Ferrara X-ray facility has already been used for the ground calibration of the JEM-X (Joint European Monitor for X-rays) detectors on board the INTEGRAL satellite (Loffredo et al., 2003), allowing the scanning of the JEM-X detection area with a pencil beam of almost monochromatic energy of value selectable in the major part of the instrument passband (3–60 keV). This scanning has permitted us to derive an accurate response function of the instrument.

Here we describe the current configuration of the Ferrara X-ray facility, its expansion now in progress and its prospects.

2. Current configuration of the X-ray facility

Figure 1 shows a sketch (not to scale) of the current configuration of the X-ray facility (Loffredo, 2004). The main components include two alternative X-ray tubes as sources of polychromatic X-ray beam: one working at lower energies (6–60 keV) and the other at higher energies (15–140 keV), a hybrid vacuum-helium system with vacuum tubes and an helium box where a fixed-exit double-crystal monochromator is installed, a system of collimators plus a Pb shield to stop the scattered radiation in the testing room, a four-axis table used as sample holder, and a three-axis table as detector holder.

2.1. X-RAY SOURCES

Two X-ray sources are available. They consist of two X-ray tubes, with different operational voltage, mounted onto an optical table and powered by independent high-voltage supplies. By means of manipulators both tubes can be moved up and down and translated along a direction perpendicular to the X-ray beam. The minimum step size is $8 \mu\text{m}$ for horizontal translations, $24 \mu\text{m}$ for vertical motions and $30''$ for rotations around the vertical axis. One of the tubes is equipped with a molybdenum anode, with its voltage which can be varied from 20 to 60 kV and the circulating current from 10 to 60 mA. The other tube is equipped with a Tungsten anode, with its voltage which can be set in the range from 40 to 140 kV and its current from 0.1 to 5 mA. The X-ray output window of the first tube is equivalent

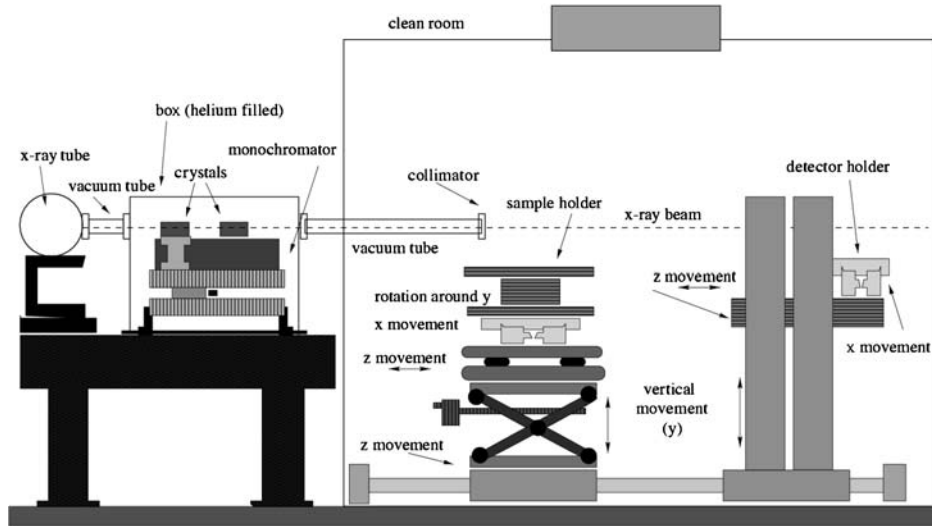


Figure 1. Sketch (not to scale) of the recent configuration of the Ferrara X-ray facility. From the left: the X-ray tube, the monochromator system, the sample holder and the detector holder. The X-ray beam travels partially within an evacuated tube and partially in a helium atmosphere.

to a 0.3 mm thick Beryllium foil, while that of the second tube is equivalent to a 1.5 mm thick aluminum foil. The window thickness fixes the low-energy threshold of the X-ray beam: about 6 keV for the first tube, 15 keV for the second.

2.2. MONOCHROMATOR

The continuum spectra provided by either X-ray tube is monochromatized with a double crystal diffractometer. The principle of operation of the monochromator and its advantages are discussed by Mills and King (1983). One of its main features is that it provides a fixed-exit beam independently of the photon energy selected. Three geometrical configurations of the reflecting crystals are possible with this fixed-exit monochromator: monolithic Bragg–Bragg (BB) channel cut, monolithic Laue–Bragg (LB) and fixed exit Bragg–Bragg (BB). The monolithic channel-cut makes use of a large single crystal. This is done by cutting a groove in a crystal parallel to the desired diffracting planes. Thus, the two crystals (actually the two opposite sides of the groove) remain parallel at all times due to the remaining material. There are, however, two distinct drawbacks to monolithic channel cut: spurious reflections and variations in exit height (offset) of the monochromatic output beam. An obvious strategy to overcome these two problems is to use two independent crystals as diffracting elements. In the Laue–Bragg configuration the crystal is cut in the shape of “L” and mounted such that the axis of rotation is at the intersection of the Bragg crystal with the Laue crystal, see Figure 2. An interesting aspect of this arrangement is that the exit beam is fixed with respect to the incident beam

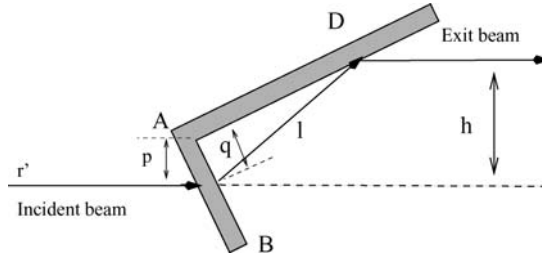


Figure 2. Top of view of the Laue-Bragg monolith configuration: A is the rotation axis, p is the distance between the incident beam and the rotation axis, D is the point where the beam is reflected and h is the distance between the incident and the exit beam.

with displacement $h = 2 \times p$, where p now is the perpendicular distance of the axis of rotation from the incident beam.

The Bragg-Bragg fixed exit monochromator replaces the Laue reflection crystal in the monolith with a crystal in the Bragg geometry that is allowed to translate. This translation is radial with respect to the axis of rotation but constrained such that the crystal remains in the path of the incident beam. The second element can be one long single crystal or a much shorter crystal that is also allowed to translate radially so long as it intercepts the beam diffracted from the first crystal, as Figure 3 shows. So the fixed-exit property of the LB monochromator is duplicated with two crystals in a Bragg reflection geometry. The diffractometer of the Ferrara X-ray facility adopts the Bragg-Bragg fixed-exit configuration: it makes use of two parallel crystal analyzers, each giving rise to a symmetric Bragg reflection. The first crystal (No. 1) has the role of selecting the desired wavelength from the incident continuum beam, while the second crystal (No. 2) re-directs the monochromatized radiation along a direction parallel to the incident beam (Loffredo et al., 2003). The diffractometer is tunable over a wide range of X-ray energies (7–120 keV), by rotating the crystals 1 and 2 and translating the crystal 2 along the direction parallel to its external surface. The system has also the capability of working in either an air or helium and it allows also the quick interchange of optical elements. With this capability the monochromator can be used with other crystals, synthetic structures,

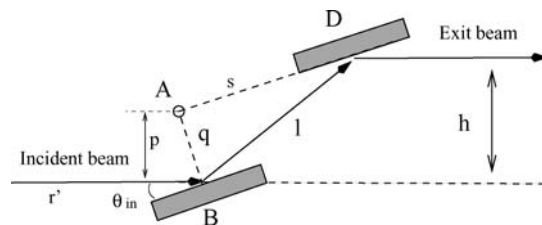


Figure 3. Top of view of the Bragg-Bragg fixed exit configuration: A is the rotation axis, θ_{in} is the Bragg angle and $h = 2 \times p$.

crystal bending, cooling devices and in general a variety of diffracting elements and mechanisms.

In order to maximize the brightness of the monochromatized beam, mosaic crystals are the best solution. We make use of Si(111) crystals with a mosaic structure of 30'' spread for a small depth of their thickness. Mosaic crystals are formed by a large number of small perfect crystallites of microscopical or submicroscopical size which are misaligned with each other (Ohler et al., 1997). They show a much wider even if lower diffraction profile when compared with perfect crystals. In general it is assumed that the crystallites are misaligned with respect to the crystal surface (for the Bragg case) following a Gaussian distribution with full-width-at-half-maximum (FWHM) β , called mosaic spread or mosaicity of the crystal. The best performance of these crystals is obtained in reflection configuration.

2.3. X-RAY BEAM PATH ENVIRONMENT

To decrease the X-ray absorption due to the air along the beam path, two devices are adopted. The first device is that of placing the monochromator within a sealed plexiglass box, where helium is pumped. With a mass-spectrometer, the amount of helium in the box can be checked. In general it is found to be $\sim 90\%$ of He and $\sim 10\%$ of air. The monochromator is tunable over a wide range of X-ray energies (7–120 keV). Because of the X-ray beam path in the plexiglass box is 200 cm, the X-ray transparency of the 100% of air at the lower working energy (7 keV) is $\sim 74\%$, while at the same energy the X-ray transparency of the mixture of $\sim 90\%$ of He and $\sim 10\%$ of air is about 96% which is enough for our purposes. The X-ray entrance and exit window of the helium box are made of polyethylene terephthalate (PET) 75 μm thick with a very high transparency at the operation energies. Outside the helium box, the X-ray beam travels in evacuated tubes (10^{-3} mbar) up to the position of the sample to be tested.

2.4. CLEAN ROOM

Both the detector and sample holders are located within a clean room of class better than 100,000. The room floor is covered with a conductive layer with a resistance of about $10^6 \Omega$ to avoid electric discharges.

2.5. SAMPLE AND DETECTOR HOLDERS

The sample holder can be moved in three perpendicular directions (X, Y, Z) and rotated around the vertical axis. The minimum step size of the translation stages is 1 μm , with linear speed from 0.025 to 8 mm/s. The travel stages are 300 mm long. The holder can support a sample of about 100 kg. The above movements are monitored with an external system of optical encoders of 5 μm sensitivity. In this way the true position of the sample and the performances of the XYZ table can be

accurately measured. The angular deformation of the table during the movement of the sample on the horizontal stage perpendicular to X-ray beam is $\leq 6''$. The angular stage has a repeatability of $1''$.

The detector holder can only be moved in three perpendicular directions (X, Y, Z), with minimum step size of the translation stages that is similar to that of the sample holder.

Both the sample and the detector holders are mounted on two separate platforms that can translate on a rail. The current length of the rail is 2.5 m.

2.6. COLLIMATION OF X-RAY BEAM

The goal of the collimation system is that of almost parallelize the X-ray beam coming from the X-ray source after its monochromatization. In order to absorb the unwanted X-rays, the material chosen for the collimators is lead or tungsten with enough thickness (at the working energies of the facility the shield is 4 mm). By changing the aperture of the collimators the divergence of the beam can be increased or decreased depending on the beam divergence tolerated. The divergence of the beam influence the energy resolution of the monochromatized beam. Indeed the reflection by the silicon crystals of the monochromator system does not completely monochromatize the beam, so the collimators after the monochromator are also needed to get the needed energy width of the monochromatized beam. The X-ray facility has two collimators fixed to the table of the monochromator. As the fine focus of the X-ray tubes has a size of about 5×5 mm the pinholes of the collimators are very narrow. Generally the aperture of the collimators depends on the kind of experiment to be performed. For example with a CZT detector which has the window of 5×5 mm, when it is positioned on the detector holder, the pinhole of the second collimator is selected at $0.5 \text{ mm} \times 0.5 \text{ mm}$, otherwise the cross section of the beam is bigger than the detector's window. The measurements show that for a required X-ray beam of $1 \text{ mm} \times 1 \text{ mm}$ at the first moving table, the second collimator must be $0.3 \text{ mm} \times 0.3 \text{ mm}$. The first collimator does not influence the size of the beam because the distance between the two collimators is too big ($\sim 1 \text{ m}$) but it influences the beam intensity. Indeed the polychromatic beam has a very big intensity (several hundred of thousand of counts to sec at working energies at the sample) which can be dangerous for our detectors, so it needs to narrow the collimators. Instead the monochromatic beam is much weaker (10–20 counts to sec at lower working energies at the sample) than the polychromatic and generally the aperture of the second collimator is $\geq 0.3 \text{ mm} \times 0.3 \text{ mm}$.

2.7. DETECTORS

A set of detectors is available for the X-ray facility. They include three NaI(Tl) scintillators, one of which is an imager, a Cadmium Zinc Telluride (CZT) and high purity germanium detector (HPGe). One of the two NaI(Tl) non-imagers has a

thickness of 4 mm with an X-ray entrance window of 0.2 mm Al, and an energy resolution of about 15% at 122 keV. The other NaI(Tl) non-imager detector has a 1 in. diameter and thickness and is mainly used to evaluate the beam intensity. The NaI(Tl) imager has a square shape with a side of 42 mm and a thickness of 3 mm. The crystal is viewed by a PMT with a two-dimensional readout. Details on this detector configuration can be found elsewhere (Poulsen et al., 1991). It is used for locating the beam position.

The CZT X-ray detector, Peltier-cooled to 250 K, is used to monitor the intensity and the spectrum of the pencil beam incident on the sample to be tested; in the case of reflectivity measurements, it is used also to measure intensity and spectrum of the diffracted beam. The CZT has the advantage of being compact and highly efficient to the beam photon energies selected. In addition it shows a very good energy resolution (0.94 keV at 60 keV). The CZT is supplied by Amptek (XR-100T-CZT model). Its cross section is 5 mm \times 5 mm, its thickness 2 mm, while its X-ray entrance window is made of a 0.25 mm thickness beryllium layer.

The high purity germanium detector (HPGe), cooled with liquid nitrogen, has a surface area of about 78.5 cm², a thickness of 13 mm and an X-ray entrance window of 0.254 mm Beryllium thickness. This configuration gives an high detection efficiency to the X-rays provided by the facility. The energy resolution is about 0.44% at 122 keV.

As an example, Figure 4 shows the spectrum, detected with the CZT detector, of the monochromatized X-ray beam with nominal energy of 17.4 keV.

The centroid energy of the monochromatized photons obtained with the X-ray facility, as measured with the CZT detector, are nicely consistent (within 1 keV) with those expected from the Bragg law (see Figure 5). The small discrepancies

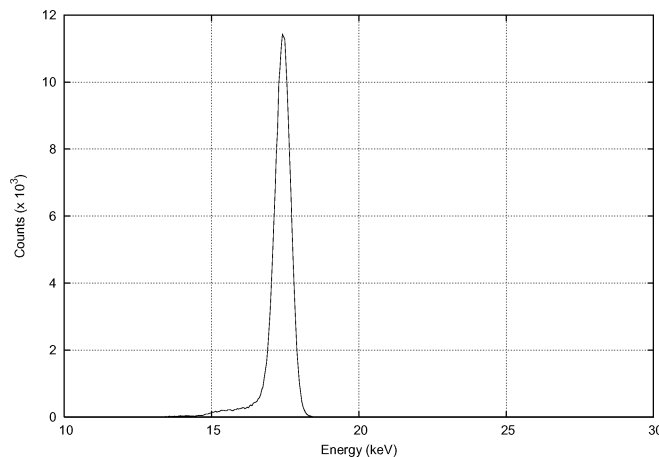


Figure 4. Spectrum of the monochromatized X-ray beam at 17.4 keV, which was available for the JEM-X calibration.

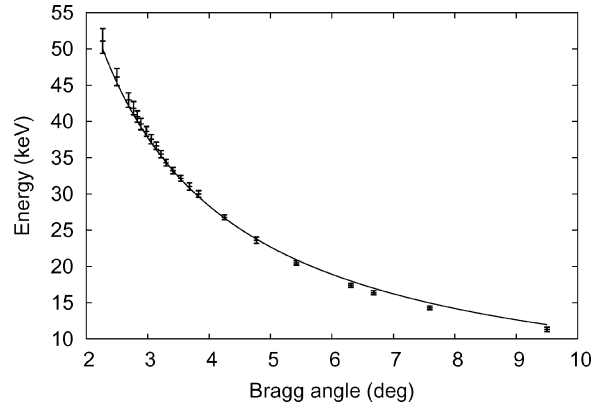


Figure 5. Energy measured of the X-ray beam as a function of the Bragg angle of the crystal No. 1 of the double-crystal monochromator. The expected energy, derived from the Bragg law, is also shown.

between measured and expected values are due to the motor positioning accuracy of the monochromator system.

2.8. SOME APPLICATIONS OF THE X-RAY FACILITY

In addition to the ground calibration of the JEM-X detectors, as mentioned before, the facility in the current configuration has been used to measure the X-ray transparency of the mask support panel of the IBIS telescope (Ubertini et al., 2004), and is now being used for reflectivity measurements of crystal samples of Cu(111) in Laue configuration within the development project of a hard X-ray focusing optics (Pellicciotta et al., in press; Pisa et al., in press). An example of reflectivity measurement of a mosaic crystal sample of Cu(111) expected to be used as reflecting material in a Laue lens (Pellicciotta et al., in press) under development is shown in Figure 6.

3. Upgrading of the facility now in progress

In the context of the development project of a Laue lens (Pisa et al., in press), a key task is the measurement of the optical axis, in hard X-rays, of many crystals tiles of Cu(111) used for the lens. Part of these measurements are expected to be performed at the Institute Laue–Langevin and part in our X-ray facility. To this end the facility is being extended and improved in order to determine the optical axis of the Cu(111) tiles with an accuracy of less than 10 arcsec (see Figure 7). The rail on which the platforms on which the sample and the detector holders are mounted, will be extended from 2.4 m up to 12 m. The rail extension will meet the requirements for an accurate crystal axis determination.

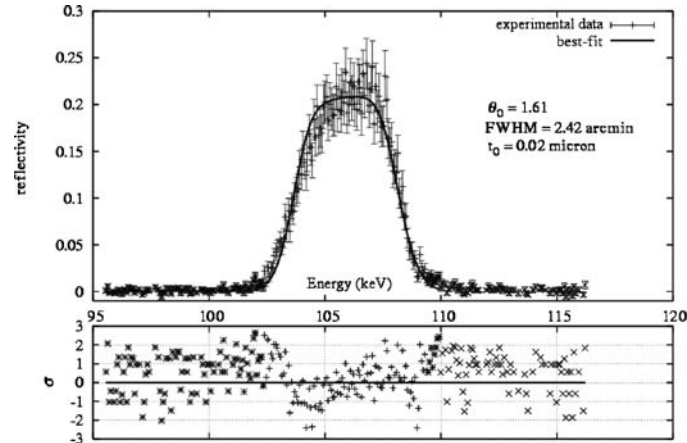


Figure 6. Reflectivity curve of a Cu(111) mosaic crystal sample in transmission configuration (Laue geometry) at about 90 keV. The best fit curve and parameters of the model function to the data are also shown: θ_0 is the Bragg angle, FWHM is the full width half maximum of the reflectivity curve and t_0 is the average thickness of the microcrystals of the mosaic crystal.

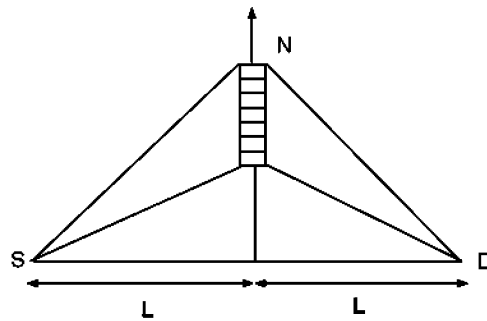


Figure 7. Crystal axis determination concept. For a crystal with lattice planes parallel to the SD direction, the X-rays from the source S are focused into the center of the detector D. If the lattice plane axis is misaligned, the focus is displaced. By means of manipulators the axis can be re-adjusted.

The sample holder will be equipped with two high precision motorized goniometers for the rotation of the sample in two orthogonal directions in the horizontal plane. With these goniometers an angular position accuracy of $3''$ can be achieved. The detector platform will be equipped with a rotation stage to orient detector axis along the direction perpendicular to the X-ray reflected beam. The resolution of this stage is $3.6''$.

The set of detectors is being enriched with an X-ray Image Intensifier viewed from a CCD camera with 1000×1000 pixels with digital video output. The intensifier has a useful entrance field size of 215 mm diameter, an X-ray detection efficiency of about 65% at 59.5 keV and a position resolution of 0.2 mm. The detector will be centered in the focal point D of Figure 7.

The extended facility will be located in one of the experimental rooms of the new LARge International X-ray laboratory (LARIX, see below).

4. Future prospects

A scientific-technological campus has already been built by the University of Ferrara, where in a short time the Physics Department and its related laboratories will move to. In this new site, also the LARIX lab is located. It consists (see Figure 8) of a 100 m long tunnel with two large experimental rooms, one of 20 m long, and the other 7 m. The larger experimental room (no. 1) will host the extended X-ray facility above described.

One of the key goals of the LARIX lab is to install inside it a large hard X-ray facility for test and calibration of hard X-/gamma-ray focusing optics or detectors. In the current design, the X-ray sources will be located in the smaller room (no. 2), while focusing optics to be tested will be located in the larger room. The 100 m long tunnel, where a beam line will be installed, will allow a small divergence of the X-ray beam.

The focusing optics (or detector) to be tested will be positioned in a large vacuum chamber (3 m diameter) already available. In the case of an X-ray optics, the reflected beam will be detected in its focal plane with suitable detectors. To this end, a shorter beamline will connect X-ray optics chamber with the detector chamber. The length of this beam line will be adjusted in order to match the X-ray optics focal length.

The LARIX lab will be addressed not only to astrophysical applications. Other applications, like fundamental physics, material science, medical physics, are also foreseen. Apparatus devoted to medical physics will be also installed in the lab.

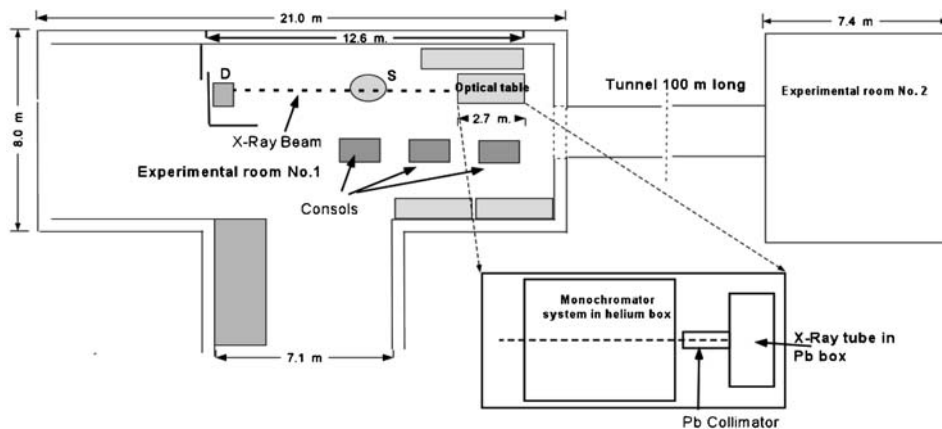


Figure 8. A view of the LARIX lab with the extended X-ray facility location shown.

References

- Fiore, F. et al.: HEXIT-SAT: A mission concept for x-ray grazing incidence telescopes from 0.5 to 70 keV. SPIE Proc. **5488**, 39–48 (2004) (astro-ph/0407647)
- Loffredo, G.: The Ferrara X-Ray Facility, Its Applications and Prospects, PhD thesis (2004)
- Loffredo, G., et al.: A&A **411**, L239 (2003)
- Mills, D.M., King, M.T.: Nucl. Instr. Methods **208**, 341 (1983)
- Ohler, M., et al.: Nucl. Instr. Methods **B129**, 257–260 (1997)
- Pellicciotta, D., et al.: IEEE Trans. on Nucl. Sci. (in press)
- Pisa, A. et al.: Feasibility study of a Laue lens for hard X-rays for space astronomy. SPIE Proc. **5536**, 933–943 (2004) (astro-ph/0411574)
- Poulsen, J. M., Verbeni, R., Frontera, F.: Position-sensitive scintillator detector for hard X-rays. Nucl. Instr. Meth. **A310**, 398–402 (1991)
- Takahashi, T. et al.: Wide band X-ray Imager (WXI) and Soft Gamma-ray Detector (SGD) for the NeXT Mission. SPIE Proc. **5488** (2004) (astro-ph/0410402)
- Ubertini, P., et al.: A&A **411**, L131 (2004)